Ultrafast excited-state dynamics in photochromic *N*-salicylideneaniline studied by femtosecond time-resolved REMPI spectroscopy

Chie Okabe
Department of Chemistry, Faculty of Science, Kyushu University, 6-1-10 Hakozaki, Higashi-ku, Fukuoka 812-8581, Japan

Takakazu Nakabayashi
Research Institute for Electronic Science, Hokkaido University, Sapporo 060-0812, Japan

Yoshiya Inokuchi
The University of Tokyo, Komaba, Meguro-ku, Tokyo 153-8902, Japan

Nobuyuki Nishi
Institute for Molecular Science, Myodaiji, Okazaki 444-8585, Japan

Hiroshi Sekiya[a)]
Department of Chemistry, Faculty of Science, Kyushu University, 6-1-10 Hakozaki, Higashi-ku, Fukuoka 812-8581, Japan

Ultrafast processes in photoexcited *N*-salicylideneaniline have been investigated with femtosecond time-resolved resonance-enhanced multiphoton ionization spectroscopy. The ion signals via the $S_1(n,\pi^*)$ state of the enol form as well as the proton-transferred *cis*-keto form emerge within a few hundred femtoseconds after photoexcitation to the first $S_1(\pi,\pi^*)$ state of the enol form. This reveals that two ultrafast processes, excited-state intramolecular proton transfer (ESIPT) reaction and an internal conversion (IC) to the $S_1(n,\pi^*)$ state, occur on a time scale less than a few hundred femtoseconds from the $S_1(\pi,\pi^*)$ state of the enol form. The rise time of the transient corresponding to the production of the proton-transferred *cis*-keto form is within 750 fs when near the red edge of the absorption is excited, indicating that the ESIPT reaction occurs within 750 fs. The decay time of the $S_1(\pi,\pi^*)$ state of the *cis*-keto form is 8.9 ps by exciting the enol form at 370 nm, but it dramatically decreases to be 1.5–1.6 ps for the excitation at 365–320 nm. The decrease in the decay time has been attributed to the opening of an efficient nonradiative channel; an IC from $S_1(\pi,\pi^*)$ to $S_1(n,\pi^*)$ of the *cis*-keto form promotes the production of the *trans*-keto form as the final photochromic products. The two IC processes may provide opposite effect on the quantum yield of photochromic products: IC in the enol form may substantially reduce the quantum yield, but IC in the *cis*-keto form increase it. © *2004 American Institute of Physics.* [DOI: 10.1063/1.1801991]

I. INTRODUCTION

Photochromism is characterized by a light-induced reversible reaction of a chemical species. This reaction gives rise to the formation of photoisomers whose electronic absorption spectra are fairly different from those of the reactant molecules, resulting in a dramatic color change of a crystal or solution. A lot of photochromic materials have received great attention to their applications to optoelectronic devices.[1–8] Among them *N*-salicylideneaniline (SA) is one of the most extensively studied photochromic molecules.[9–31]

Figure 1 displays the change in the geometry of SA after photoexcitation of the enol form. Density functional theory calculation at the B3LYP/6-31G** level predicts that the relative energy of the enol form is 5520 cm^{-1} lower than the *trans*-keto form.[31] Over the past few decades, a considerable number of experimental and theoretical studies have been

devoted to clarify the mechanism of photochromic reaction of SA.[9–31] Different precursors and processes have been proposed to explain the photochromism of SA. A common feature of the photochromic reaction of SA derived from recent studies is summarized as follows.[25–28,30,31] The excited-state intramolecular proton transfer (ESIPT) followed by photoexcitation of the enol form to its first $^1(\pi,\pi^*)$ state $[S_1(\pi,\pi^*)]$ produces the $S_1(\pi,\pi^*)$ state of the *cis*-keto form, leading to a metastable *trans*-keto form as the final photoproduct. However, the detailed mechanism of the photochromic reaction of SA is controversial, in particular the depopulation processes after ESIPT are ambiguous. Picosecond and nanosecond time-resolved measurement of SA in low-temperature matrices suggests that the precursor of the photochromic species is a vibrationally "hot" proton-transferred *keto*-form.[15] A similar transient is proposed from femtosecond and picosecond time-resolved measurements of SA in various solutions at room temperature.[15,25–27] Mitra and Tamai estimated the time constant for the transition from the vibrationally hot state of the *cis*-keto form to the *trans*-
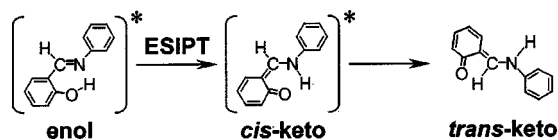
FIG. 1. Stable structures and photochromic reaction of SA.

FIG. 2. Schematic diagram of the femtosecond time-resolved REMPI spectroscopy. Nd:YVO$_4$, diode-pumped cw Nd:YVO$_4$ laser; Ti:Sapphire, femtosecond mode-locked Ti:sapphire laser; YLF, *Q*-switched cw Nd:YLF laser; RGA, femtosecond regenerative amplifier; OPA, optical parametric amplifier; SHG, second harmonic generator; VD variable optical delay line; MSP, microsphere plate; PC, personal computer.

keto form to be 300–400 fs.[25–27] Zgierski and Grabowska carried out theoretical calculations on SA (Ref. 30) and related molecules[32–34] to investigate the geometries of tautomers, the transition energies, the rate for ESIPT, and the precursor of the photochromic species. They proposed that the common precursor of the final photochromic species and the fluorescent species is the vibrationally excited $S_1(\pi,\pi^*)$ state of the enol form, and the formation of the *trans*-keto form as the final photochromic products can be explained without considering the vibrational hot *keto*-form as a reaction intermediate.

In the present work we focus on ultrafast processes in the proton-transferred *cis*-keto form as well as those in the enol form. Recently, we reported the laser-induced fluorescence (LIF) and dispersed fluorescence spectra of jet-cooled SA.[31] The onset of the $S_1(\pi,\pi^*) \leftarrow S_0$ absorption has been found to lie below 400 nm, and no vibrationally resolved structure was observed. A very broad feature in the LIF spectrum suggests that an ultrafast nonradiative process occurs in addition to the ESIPT reaction after photoexcitation to the $S_1(\pi,\pi^*)$ state. This ultrafast process may significantly influence the excited-state dynamics and the quantum yield of the photochromic products, but this process has not been observed.

As described above conclusive results have not been obtained to elucidate the photochromic reaction of SA. Femtosecond real-time probing of the excited states in a molecular beam is crucial for complete understanding of the ultrafast processes in SA. Numerous studies have been carried out to reveal the photoexcited dynamics of SA in the condensed phase.[9–20,22,23,25–29] However, the solvent effect may significantly influence the excited-state dynamics of SA in the condensed phase, because a large change in the geometry occurs during the photochromic reaction of SA. The ESIPT rate and the quantum yield for the photochromic products substantially depend on the nature of the solvent molecules.[25,26] Spectral changes due to intermolecular vibrational relaxation as well as solvation make it difficult to determine the time constants in solution by ultrafast optical spectroscopy.[27] Therefore, the investigation of the ultrafast processes under the gas phase condition, where the solvent effect is absent, is desired to obtain inherent nature of the electronic states of SA. Ultrafast intramolecular processes proceed on the femtosecond to picosecond time scale.[25–27,35–43] Since the quantum yield of photochromic reaction is defined as the ratio of the rate for the photochromic process to that for the other processes, the femtosecond time resolution is crucial to clarify the excited state dynamics of the photochromic compounds. Resonance-enhanced multiphoton ionization (REMPI) technique is very useful to investigate nonradiative processes.[37,39–43]
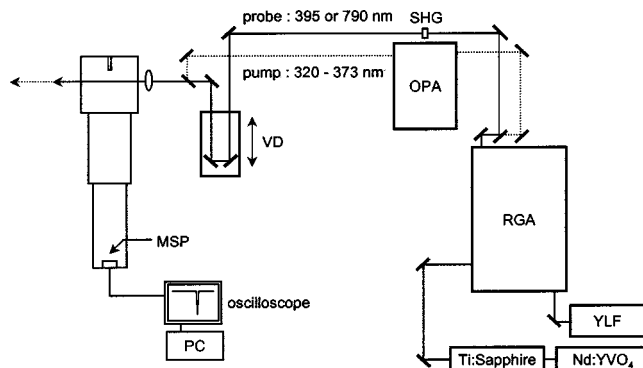
We apply the femtosecond time-resolved REMPI technique to investigate the real-time dynamics after photoexcitation of the enol form under the jet-cooled conditions. The electronic excited states of the enol and *cis*-keto forms are selectively ionized by choosing the pump and probe wavelengths. Two rapid internal conversion (IC) processes have been observed for the first time: one is IC from the $S_1(\pi,\pi^*)$ state to the $S_1(n,\pi^*)$ state of the enol form and the other is IC from the $S_1(\pi,\pi^*)$ state to the $S_1(n,\pi^*)$ state of proton-transferred *cis*-keto form. The role of the two IC processes in the photochromic reaction of SA has been discussed.

II. EXPERIMENT

The experimental setup for femtosecond time-resolved REMPI spectroscopy is drawn in Fig. 2. A femtosecond Ti:sapphire laser (Spectra Physics, Tsunami) was pumped by a diode laser (Spectra Physics, Millennia). The output pulses from the Ti:sapphire laser were used to seed a regenerative amplifier (Spectra Physics, Spitfire) pumped by a frequency-doubled Nd:YLF laser (Spectra Physics, Merlin) to generate amplified pulses with ~1 mJ/pulse at a repetition rate of 1 kHz. The amplified output was split into two beams. A part of the amplified output beam (0.85 mJ/pulse) was used to excite an optical parametric amplifier (OPA) system (Spectra Physics, OPA-800). The fourth harmonic of the signal wave (320–373 nm) was used as a pump beam. Two different wavelengths, the fundamental (790 nm) and the second harmonic (395 nm) of the remainder of the amplified output (0.15 mJ/pulse), were used as a probe beam. The power densities used for the pump and probe lasers were ≈1 $\times 10^{-10}$ W/cm^2 and ≈1 $\times 10^{-11}$ W/cm^2, respectively. The probe beam was optically delayed with respect to the pump beam using a computer-controlled delay stage. The pump and probe beams were superimposed by a dichroic mirror, and loosely focused into a vacuum chamber with a 350 mm focal lens. Both of the pump- and probe-pulse energies were strongly reduced to avoid saturation and interference from higher order multiphoton excitation. The average pulse energy at the entrance of the chamber was ~500 nJ for the
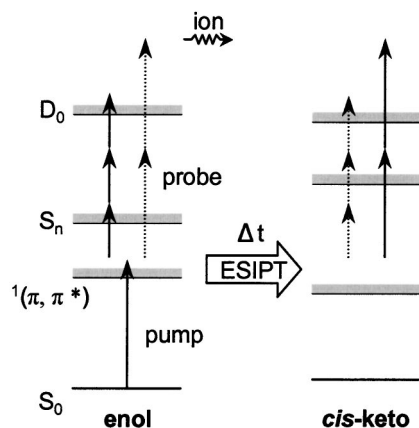
FIG. 3. Energy diagram and ionization scheme for the enol and *cis*-keto forms of SA. The probe wavelength of $\sim$400 nm is resonant with the S_n-S_i transition of the *cis*-keto form. Resonant wavelength for the S_n-S_1 transition of the enol form may be longer than 700 nm.

pump pulse, 4 μJ and 40 μJ for the 395 and 790 nm probe pulses, respectively. The FWHM of the response function was $\sim$240 fs. The product ions were mass analyzed in a time-of-flight mass spectrometer and detected using a microsphere plate. The ion signals were fed into a digital storage oscilloscope. The integrated intensity of the parent ion signal was recorded as a function of the delay time between the pump and probe pulses. SA vapor at 350 K was seeded in He gas at 1 atm, and the mixture was expanded into the vacuum chamber through a cw nozzle. SA was purchased from Tokyo Kasei and used as received. The OH-deuterated derivative was obtained by introducing D_2O into the nozzle housing.

III. RESULTS

A. Two different photoionization processes in SA

Figure 3 shows an ionization scheme for the enol and *cis*-keto forms of SA. The enol form is excited to the $S_1(\pi,\pi^*)$ state with the pump pulse, and subsequently ionized with the probe pulse. The time evolution of photoexcited molecules can be obtained by monitoring the ion signals as a function of the delay time between the pump and probe pulses. Since the ion intensity largely depends on the resonance condition, the selective ionization of the enol or *cis*-keto form in the excited state can be achieved by choosing the wavelength of the probe beam. In solution the enol form shows a broad $S_n \leftarrow S_1$ absorption in the range of 400–500 nm, while the *cis*-keto form shows a sharp and strong $S_n \leftarrow S_1$ absorption with a maximum at around 420 nm.[25–27] Thus, the second harmonic of Ti:sapphire laser is useful to ionize the *cis*-keto form in the S_1 state selectively.

To examine the selectivity of the ionization for the enol and keto forms, we have measured the time profiles of the ion signal intensity of photoexcited SA with several probe wavelengths. Figures 4(a) and 4(b) show the time profile of the ion signal of SA by using the probe wavelengths of 790 and 395 nm, respectively. The pump wavelength is 320 nm in both the cases. Figures 5(a) and 5(b) show the relative ion intensities as a function of the square of the power density probed at 390 nm and the cube of the power density probed
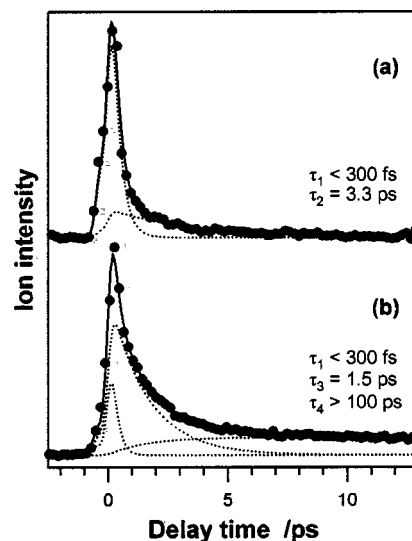

FIG. 4. Decay profiles of SA excited at 320 nm and probed at (a) 790 nm and (b) 395 nm. The solid circles are experimental data, while the solid curves are the best-fitted curves obtained by two or three decay components. The dotted curves represent the components used to decompose the decay profiles.

at 790 nm, respectively. In Figs. 5(a) and 5(b) the ion intensity increases linearly with the square of the power density and the cube of the power density, respectively. These data show that the photoionization of SA takes place by absorbing one pump photon and three probe photons, i.e., $(1+3')$ process, for the pump wavelength at 320 nm and the probe wavelength at 790 nm. However, the photoionization occurs via the $(1+2')$ process with the probe wavelength at 395 nm.

The time dependence of the ion intensity markedly depends on the probe wavelength used (see Fig. 4). The decay
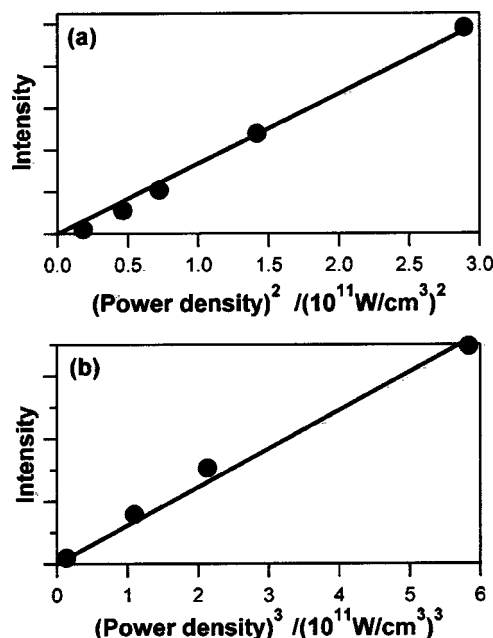

FIG. 5. Probe power dependence of the ion intensities of SA exciting at 320 nm. The relative ion intensities probed at 395 nm are plotted as a function of the square of the power density in (a), while those probed at 790 nm are plotted as a function of the cube of the power density in (b).
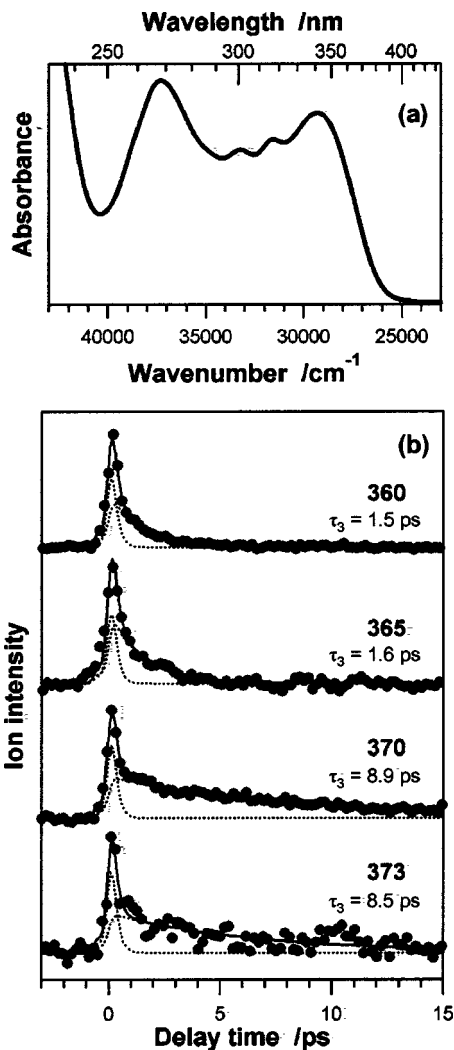
FIG. 6. (a) Electronic absorption spectrum of SA in *n*-hexane solution. (b) Decay profiles of SA measured by varying the pump wavelength from 360 to 373 nm, while probing at 395 nm. The pump wavelength is given on the right-hand side of each time profile. The solid circles are experimental data, while the solid curves are the best-fitted curves obtained by biexponential decay components.

TABLE I. Best-fit time constants of SA in units of ps obtained from femtosecond time-resolved measurement. τ_1 and τ_2 are time constants obtained from the decay profiles of $S_1(\pi,\pi^*)$ and $S_1(n,\pi^*)$ of the enol form, while τ_3 and τ_4 are time constants obtained from the decay profiles of $S_1(\pi,\pi^*)$ of the keto form.

$\lambda(\text{pump})^{\text{a}}$	$\lambda(\text{probe})^{\text{a}}$	τ_1	τ_2	τ_3	τ_4
320	790	<0.3	3.3±0.5		
320	395	<0.3		1.5±0.3	>100
360	395	<0.3		1.6±0.3	
365	395	<0.3		1.6±0.5	
370	395	<0.3		8.9±0.7	
373	395	<0.3		8.5±1.5	

[a]Wavelength of the pump and probe pulses in units of nm.

nance with the optical absorption and the probe wavelength of 395 nm. All the experimental traces are fitted by a convolution of the response function with a biexponential decay. No rise component is necessary to reproduce the time profile within the experimental accuracy; all the observed species appear within time constants of 750 fs. The decay is composed of a femtosecond component with a time constant (τ_1) of <300 fs and a picosecond one with a time constant (τ_3) of 1.5–8.9 ps. The time constants obtained from the decay profiles in Figs. 4 and 6 are summarized in Table I. The fast component decays within 300 fs and this time constant hardly depends on the pump wavelength in the range from 360 to 373 nm, while the time dependence of the slower component is sufficiently affected by the pump wavelength used.

The rise time of the slow component is almost independent of both the pump wavelength and the deuteration of the hydroxy proton within the present experimental accuracy. The rise time of the second component with the pump wavelength of 370 nm is within 750 fs in deuterated SA.

IV. DISCUSSION

A. ESIPT and IC from $S_1(\pi,\pi^*)$ of enol form

The femtosecond $(1+3')$ and $(1+2')$ REMPI measurements in this study provide new information about the ultrafast dynamics of photoexcited SA. In Fig. 4(a), two time constants ($\tau_1<300$ fs and $\tau_2=3.3$ ps) are estimated from the time profile observed with the pump and probe wavelengths of 320 nm and 790 nm, respectively. On the other hand, in Fig. 4(b), three time constants ($\tau_1<300$ fs, $\tau_3=1.5$ ps, and $\tau_4>100$ ps) are necessary to reproduce the decay profile recorded with the pump and probe wavelengths of 320 and 395 nm, respectively. A very fast decay component ($\tau_1<300$ fs) is attributed to a decay of the $S_1(\pi,\pi^*)$ state of the enol form. A component $\tau_3=1.5$ ps in Fig. 4(b) arises from the *cis*-keto form produced via the ESIPT reaction, because the probe wavelength at ~400 nm is in resonance with the S_n-S_1 transition of the *cis*-keto form.[25–27] A component $\tau_2=3.3$ ps in Fig. 4(a) is attributed to the decay of an excited state of the enol form. This state must be populated via the $S_1(\pi,\pi^*)$ state of the enol form, suggesting that an ultrafast nonradiative process occurs in addition to the ESIPT reaction. The rise time of the transient corresponding to the production of the $S_1(n,\pi^*)$ is estimated to be within 500 fs.
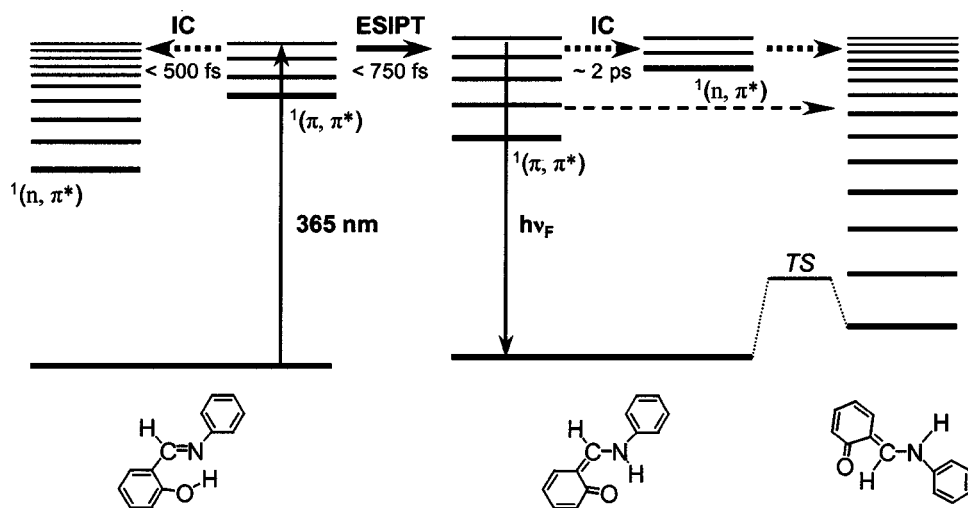
profile in Fig. 4(a) is well reproduced by a convolution of the response function with a biexponential decay, giving time constants of $\tau_1<300$ fs and $\tau_2=3.3$ ps. On the other hand, the decay profile in Fig. 4(b) cannot be fitted with a biexponential function. The decay profile in Fig. 4(b) is well fitted using a triexponential decay function with time constants of $\tau_1<300$ fs, $\tau_3=1.5$ ps, and $\tau_4>100$ ps. As mentioned above, the difference in the decay profiles in Figs. 4(a) and 4(b) is attributable to the difference in the ionization efficiency for the enol and keto forms. The assignment of these time components will be discussed in detail in Sec. IV.

B. Excitation wavelength dependence of decay processes

Figure 6(a) shows the absorption spectrum of SA in *n*-hexane. The absorption onset of SA is located at 380–400 nm, and two absorption maxima are seen at 270 and 340 nm. Figure 6(b) shows the femtosecond time-resolved REMPI intensities observed with several pump wavelengths in reso-

FIG. 7. Photoexcited processes of SA drawn on the basis of the femtosecond time-resolved REMPI spectroscopy in gas phase. Two ultrafast processes ES-IPT and IC occur by photoexcitation of a high vibronic state of the enol form. When the pump wavelength is shrorter than ~365 nm, an IC occurs from the $^1(\pi,\pi^*)$ to the $^1(n,\pi^*)$ state of the proton-transferred *cis*-keto form in addition to the radiative ($h\nu_F$) and nonradiative decay to the S_0 state. The IC efficiently produces the *trans*-keto form as the final photochromic products. The *trans*-keto form may be produced as a minor channel when the enol form is excited at wavelength longer than 370 nm. TS indicates a transition state.

The existence of the two ultrafast decay processes from the $S_1(\pi,\pi^*)$ state of the enol form is consistent with the results of our previous study.[31] A very broad feature in the LIF spectrum was attributed to the existence of a very rapid nonradiative process other than the ESIPT reaction. The LIF spectrum of SA in a free jet expansion indicates that the energy difference between the first $^1(\pi,\pi^*)$ state and the S_0 state is smaller than 25 000 cm^{-1}. *Ab initio* calculation at the HF/6-31G* level indicates that the stable ground state geometry of the enol form is achieved by twisting the anilino ring by ~44° at the HF/6-31G* level.[30] The excitation of the enol form in a higher vibronic state in $^1(\pi,\pi^*)$ may generate a planar molecule (C_s) that can undergo the ESIPT reaction. Zgierski and Grabowska predicted that the first $^1(n,\pi^*)$ state with C_s symmetry is located slightly above the $S_1(\pi,\pi^*)$ state, but the $S_1(n,\pi^*)$ state with C_1 geometry produced by IC from the $S_1(\pi,\pi^*)$ state may be stabilized by twisting the two carbon rings by ~94° and the $S_1(n,\pi^*)$ state with C_1 geometry is predicted to be lower than the $S_1(\pi,\pi^*)$ state.[30] The observation of a second ultrafast process is consistent with the broad feature in the LIF spectrum[31] and the results of theoretical calculations.[30] Thus, $\tau_2 = 3.3$ ps in Fig. 4(a) is attributed to the decay of $S_1(n,\pi^*)$ of the enol form.

The geometry of the enol form may change from planar to nonplanar accompanying with the IC process from $S_1(\pi,\pi^*)$ to $S_1(n,\pi^*)$. When the $S_1(n,\pi^*)$ potential surface crosses the $S_1(\pi,\pi^*)$ potential surface,[30] the conical intersections may significantly promote a rapid IC.[44,45]

In Fig. 4(a) the ion signal from the $S_1(n,\pi^*)$ state of the enol form is weaker than that from the $S_1(\pi,\pi^*)$ state of the enol form. Since the $(1+3')$ process is employed for the observation of the ultrafast dynamics of the enol form, the difference in resonance condition as well as that in population should be considered to discuss the intensity difference between the two components in Fig. 4(a). We have measured the decay profile of SA using the pump and probe wavelengths of 320 and 810 nm, respectively, and found that the ion intensity from the $S_1(n,\pi^*)$ state relative to that from the $S_1(\pi,\pi^*)$ state becomes weaker with the use of the longer probe wavelength. This indicates that the weak signal

from the $S_1(n,\pi^*)$ state in Fig. 4(a) cannot be explained only by the difference in population between the $S_1(n,\pi^*)$ and $S_1(\pi,\pi^*)$ states.

B. IC from *cis*-keto form

The deactivation processes following the photoexcitation of the enol form are drawn in Fig. 7 on the basis of the results of the femtosecond time-resolved REMPI measurement together with the theoretical studies.[30,31] The diagram in Fig. 7 obtained from the experimental studies in the gas phase is in good agreement with a picture predicted from *ab initio* calculations (Fig. 4 in Ref. 30). The $S_1(n,\pi^*)$ state of the enol form and the proton-transferred *cis*-keto form are generated after the photoexcitation of the enol form to the $S_1(\pi,\pi^*)$ state. We have found that the decay time τ_3 of the $S_1(\pi,\pi^*)$ state of the *cis*-keto form dramatically changes from 1.5 to 8.9 ps with the excitation wavelength from 373 to 360 nm. The remarkable change in the decay time is reasonably explained by the existence of a threshold for the ultrafast nonradiative process from the $S_1(\pi,\pi^*)$ state of the *cis*-keto form when the enol form is excited between 370 and 365 nm.

The electronic state of the proton transferred *cis*-keto form must be a $^1(\pi,\pi^*)$ state, since the nature of the electronic state of the *cis*-keto form produced via the ESIPT reaction should be very similar to that of the enol form. Theoretical calculations predicted that the lowest (n,π^*) state of the *cis*-keto form with C_s symmetry lies somewhat higher in energy than the $S_1(\pi,\pi^*)$ state. However, the *cis*-keto form in the (n,π^*) state is significantly stabilized by a twist of the phenyl ring that becomes almost perpendicular to the anilino ring.[30]

The $S_1(n,\pi^*)$ state of the *cis*-keto form having a twisted structure plays an important role as an effective depopulation channel leading to the *trans*-keto form. The remarkable shortening of τ_3 with increasing the excitation energy is ascribed to the opening of an IC channel from the $S_1(\pi,\pi^*)$ state to the $S_1(n,\pi^*)$ state of the *cis*-keto form. The quantum yield of the photochromic products is known to be inversely proportional to the fluorescence quantum yield

of SA; the photochromic quantum yield at 334 nm excitation wavelength is three times larger than that at 365 nm, whereas the fluorescence quantum yield in solution decreases with increasing excitation energy.[13]

A long-lived decay component ($\tau_4 > 100$ ps) is detected by using the pump and probe wavelengths of 320 and 395 nm, respectively. A candidate for the species responsible for the long-lived component is a $^1(\pi, \pi^*)$ state of a second *cis*-keto form that has a nonplanar structure,[31] a high vibrationally excited state of the *trans*-keto form, and a triplet state of the proton-transferred *cis*-keto form. The existence of a second *cis*-keto isomer has been suggested both from experiment and theoretical calculations.[17,26,30,31] It is difficult to assign τ_4 from the present measurement.

C. H/D isotope effect on ESIPT

We have investigated whether the potential energy barrier exists or not in the ESIPT reaction by varying the pump wavelength between 360–373 nm with the $(1+2')$ REMPI technique. The rise time of the transient corresponding to the formation of the *cis*-keto form is less than 750 fs for the pump wavelength at 373 nm. In addition, no significant OH/OD isotope effect on the rise time is detected. These results indicate that the ESIPT reaction occurs within 750 fs and the wavelengths shorter than 373 nm excite the energy region where there is no potential barrier to proton transfer. The ESIPT time in cyclohexane is 210 fs, and it becomes longer (245–380 fs) in polar solvents.[25–27] The ESIPT time measured in this study is consistent with those obtained from the femtosecond study in solution.

The potential barrier height to proton transfer is predicted to be 3.2–7.2 kcal/mol from B3LYP/6-31G* and CIS/6-31G* calculations.[30] The calculated barrier heights do not contradict our experimental result. However, the LIF spectrum of SA in a supersonic jet expansion shows that the onset of the $S_1(\pi, \pi^*)$-S_0 absorption lies at $<25\,000$ cm^{-1} (400 nm). Owing to very small magnitude of the Franck-Condon factors for the $S_1(\pi, \pi^*)$-S_0 transition, the ion intensity enough for the analysis of the ESIPT rate was not obtained with the pump wavelength longer than 373 nm (26 800 cm^{-1}) in the present study. Therefore, we cannot immediately conclude that the potential barrier is small or no barrier in the ESIPT reaction.

D. Comparison with time-resolved studies of SA in condensed phase

The $S_1(n, \pi^*)$ state of the enol form had not been observed before this study. The present study demonstrated that the femtosecond REMPI spectroscopy is more sensitive than the transient absorption spectroscopy to detect the $S_1(n, \pi^*)$ state of SA.

The depopulation processes of the *cis*-keto form have been extensively investigated both experimentally[9–15,17,18,20,22–27,31] and theoretically.[21,24,26,30] A common subject of spectroscopic studies on SA has been *Which species is the precursor of the photochromic products*. For example, Barbara, Rentzepis, and Brus studied photochemical kinetics of SA in a low temperature matrices at 4 K.[15] They

observed a biexponential decay from the proton transferred *cis*-keto form in protic solvents; a short-lived component and a long-lived component were assigned to vibrational excited fluorescence from hot state (QA*) and fluorescence from the vibrationally relaxed state (QB*), respectively. QA* has been proposed as a precursor of the *trans*-keto form that is responsible for the photochromism. Picosecond and femtosecond studies on SA in various solutions by Mitra and Tamai obtained similar results.[25–27] They observed the vibrational relaxation process of the proton transferred *cis*-keto form in the $S_1(\pi, \pi^*)$ state with a time constant of 300–400 fs and suggested that the transition to the electronic ground state of the *trans*-keto form also occurs with a similar time constant. The observation of the hot state in the condensed phase does not contradict the present study, but the decay process in this state is not clear from the time-resolved measurements in the condensed phase.[13,25,27] In contrast, the formation process of the *trans*-keto form has been reasonably explained by measuring the excitation wavelength dependence of the decay profile of the proton-transferred *cis*-keto form in the gas phase.

The decay time of the planar *cis*-keto form is 1.5–1.6 ps for the excitation of the enol form at <365 nm and 8.5 ps at >370 nm. It should be noted that the initial state of the enol form excited at 370 nm wavelength is substantially high vibronic state where the excess energy from the zero-point level of the $S_1(\pi, \pi^*)$ state is larger than 2000 cm^{-1}. Therefore, the proton transferred *cis*-keto form must be populated in a high vibronic state. Since the two carbon rings of the *cis*-keto form are predicted to be perpendicular in the $S_1(n, \pi^*)$ state of the *cis*-keto form,[30] the twisting of the nonplanar $S_1(n, \pi^*)$ state may efficiently produce the *trans*-keto form. Thus, the formation of the *trans*-keto form has been consistently elucidated with a simple picture based on the gas-phase femtosecond time-resolved study.

V. CONCLUSION

We have applied femtosecond time-resolved REMPI technique for the investigation of the ultrafast dynamics of SA under the jet-cooled isolated conditions for the first time. On the basis of the experimental data the following conclusions have been derived: (1) the electronic excited states of the enol and *cis*-keto forms can be selectively ionized by choosing the probe wavelength at 790 nm for the enol form and at 395 nm for the *cis*-keto form. (2) Three decay components (<300 fs, 1.5 ps, and 3.3 ps) are obtained by using the pump wavelength of 320 nm and the probe wavelength of 395 nm. The obtained time constants of 3.3 ps and 1.5 ps are attributed to the decay of the enol form in the $S_1(n, \pi^*)$ state and that of the *cis*-keto form in the $S_1(\pi, \pi^*)$ state generated via the ESIPT reaction, respectively. The very fast decay component (<300 fs) is due to the two ultrafast processes, IC from $S_1(\pi, \pi^*)$ to $S_1(n, \pi^*)$ of the enol form and ESIPT. The IC time is estimated to be within 500 fs. (3) The ESIPT reaction occurs within 750 fs. (4) The decay time of the proton-transferred *cis*-keto form strongly depends on the excitation wavelength for the enol form in the range from 365 to 370 nm. This indicates that a threshold exists as an

efficient IC channel from $S_1(\pi,\pi^*)$ to $S_1(n,\pi^*)$ of the *cis*-keto form, and the IC time is estimated to be ~2 ps.

In summary, femtosecond time-resolved REMPI spectroscopy has been successfully applied to investigate the excited-state dynamics of SA. It has been found that the two ultrafast IC processes play important roles in the photochromic reaction of SA: one is IC from $S_1(\pi,\pi^*)$ to $S_1(n,\pi^*)$ of the enol form and the other is IC from $S_1(\pi,\pi^*)$ to $S_1(n,\pi^*)$ of the *cis*-keto form. The former IC reduces the quantum yield of the photochromic products, while the latter increases it.

ACKNOWLEDGMENTS

[1] M. Hirano, A. Miyashita, and H. Nohira, Chem. Lett. **1991**, 209.
[2] O. Pieroni, A. Fissi, N. Angelini, and F. Lenci, Acc. Chem. Res. **34**, 9 (2001).
[3] E. Sackmann, J. Am. Chem. Soc. **93**, 7088 (1971).
[4] H. Rau and E. Luddecke, J. Am. Chem. Soc. **104**, 1616 (1982).
[5] P. J. Darcy, H. G. Heller, P. J. Stryldom, and J. Whittall, J. Chem. Soc. [Perkin 1] **1981**, 202.
[6] Y. Yokoyama, Chem. Rev. (Washington, D.C.) **100**, 1717 (2000).
[7] M. Irie and M. Mohri, J. Org. Chem. **53**, 803 (1988).
[8] M. Irie, Chem. Rev. (Washington, D.C.) **100**, 1685 (2000).
[9] M. D. Cohen and G. M. J. Schmidt, J. Phys. Chem. **66**, 2442 (1962).
[10] R. S. Becker and W. F. Richey, J. Am. Chem. Soc. **89**, 1298 (1967).
[11] W. Ottolenghi and D. S. McClure, J. Chem. Phys. **46**, 4613 (1967).
[12] R. Potashnik and M. Ottolenghi, J. Chem. Phys. **51**, 3671 (1969).
[13] T. Rosenfeld, M. Ottolenghi, and A. Y. Meyer, Mol. Photochem. **5**, 39 (1973).
[14] R. Nakagaki, T. Kobayashi, J. Nakamura, and S. Nagakura, Bull. Chem. Soc. Jpn. **50**, 1909 (1977).
[15] P. F. Barbara, P. M. Rentzepis, and L. E. Brus, J. Am. Chem. Soc. **102**, 2786 (1980).
[16] C. J. W. Lewis and C. Sandorfy, Can. J. Chem. **60**, 1738 (1982).
[17] D. Higelin and H. Sixl, Chem. Phys. **77**, 391 (1983).
[18] R. S. Becker, C. Lenoble, and A. Zein, J. Phys. Chem. **91**, 3509 (1987).
[19] W. Turbeville and P. K. Dutta, J. Phys. Chem. **94**, 4060 (1990).
[20] T. Yuzawa, H. Takahashi, and H. Hamaguchi, Chem. Phys. Lett. **202**, 221 (1993).
[21] W. Fang, Y. Zhang, and X. You, J. Mol. Struct.: THEOCHEM **334**, 81 (1995).
[22] K. Kownacki, A. Mordzinski, R. Wilbrandt, and A. Grabowska, Chem. Phys. Lett. **227**, 270 (1994).
[23] M. I. Knyazhansky, A. V. Metelitsa, A. Ja. Bushkov, and S. M. Aldoshin, J. Photochem. Photobiol., A **97**, 121 (1996).
[24] M. E. Kletskii, A. A. Millov, A. V. Metelitsa, and M. I. Knyazhansky, J. Photochem. Photobiol., A **110**, 267 (1997).
[25] S. Mitra and N. Tamai, Chem. Phys. Lett. **282**, 391 (1998).
[26] S. Mitra and N. Tamai, Chem. Phys. **246**, 463 (1999).
[27] S. Mitra and N. Tamai, Phys. Chem. Chem. Phys. **5**, 4647 (2003).
[28] M. Y. Shen, L. Z. Zhao, T. Goto, and A. Mordzinski, J. Lumin. **87–89**, 667 (2000).
[29] M. Y. Shen, L. Z. Zhao, T. Goto, and A. Mordzinski, J. Chem. Phys. **112**, 2490 (2000).
[30] M. Z. Zgierski and A. Grabowska, J. Chem. Phys. **112**, 6329 (2000).
[31] N. Otsubo, C. Okabe, H. Mori, K. Sakota, K. Amimoto, T. Kawato, and H. Sekiya, J. Photochem. Photobiol., A **154**, 33 (2002).
[32] M. Z. Zgierski and A. Grabowska, J. Chem. Phys. **113**, 7845 (2000).
[33] M. Z. Zgierski, J. Chem. Phys. **115**, 8351 (2001).
[34] M. Z. Zgierski, A. Fernández-Ramos, and A. Grabowska, J. Chem. Phys. **116**, 7486 (2002).
[35] P. M. Felker, W. R. Lambert, and A. H. Zewail, J. Chem. Phys. **77**, 1603 (1982).
[36] J. L. Herek, S. Pedersen, L. Ban_ares, and A. H. Zewail, J. Chem. Phys. **97**, 9046 (1992).
[37] A. Douhal, F. Lahmani, and A. H. Zewail, Chem. Phys. **207**, 477 (1996).
[38] C. Lu, R. R. Hsieh, I. Lee, and P. Cheng, Chem. Phys. Lett. **310**, 103 (1999).
[39] S. Lochbrunner, T. Schultz, M. Schmitt, J. P. Shaffer, M. Z. Zgierski, and A. Stolow, J. Chem. Phys. **114**, 2519 (2001).
[40] C. Su, J. Lin, R. R. Hsieh, and P. Cheng, J. Phys. Chem. A **106**, 11997 (2002).
[41] W. Radloff, Th. Freudenberg, H.-H. Ritze, V. Stert, F. Noack, and I. V. Hertel, Chem. Phys. Lett. **261**, 301 (1996).
[42] D. Zhong, E. W.-G. Diau, T. M. Bernhardt, S. D. Feyter, J. D. Roberts, and A. H. Zewail, Chem. Phys. Lett. **298**, 129 (1998).
[43] H. Ishikawa, Y. Shimanuki, M. Sugiyama, Y. Tajima, M. Kira, and N. Mikami, J. Am. Chem. Soc. **124**, 6220 (2002).
[44] Y. Haas, M. Klessinger, and S. Zilberg, Chem. Phys. **259**, 121 (2000), preface special issue on conical intersection.
[45] A. Kuhl and W. Domcke, J. Chem. Phys. **16**, 263 (2002).